Whole-body musculo-skeletal model V1

Galo Maldonado, Philippe Souères and Bruno Watier
LAAS-CNRS, Université de Toulouse, CNRS, UPS, Toulouse, France

CONTENTS

I. Introduction

The main goal of this project was to build a basic musculo-skeletal model of the human body in order to be able of analyzing and simulating human motion. To this end, an OpenSim [4] musculo-skeletal model was modified and augmented based on previous works of the literature. The resulting model is also compatible with Pinocchio [3], an open source C++ library for efficient rigid multi-body dynamics computations based on revisited Roy Featherstone's algorithms. This allows users for creating powerful simulations of whole-body human-based motions with anthropomorphic systems. Using Pinocchio with the model permits also to use state-of-the-art libraries written in C++ or python (e.g. from robotics, machine learning, ...).

The first version of the whole-body model was modified and built based on the following specific criteria:

- The model should express the main elementary motions of humans performing parkour [11], [12].
- The model has to be used for the analysis and generation of anthropomorphic motion [13]. This implies that the model should be more complicated than a humanoid robot model for instance, but not as a complex as a complex human model.
- The model should be whole-body and three dimensional as sportive practicers require whole-body coordination for accomplishing complex motions.
- The model has to include surface joint stabilizer muscles that favor the study of muscular activity in highly dynamic motion. For example the agonist-antagonist muscles that perform abduction-adduction, flexion-extension or plantar flexion-dorsiflexion.

In the sequel we provide a technical report of the skeletal and muscular modeling. This model is freely available for download at https://github.com/GaloMALDONADO/ospi along with all the libraries to parse the model to use it with Pinocchio. Some examples of utilization and motion data are also provided.

II. Methods

In this section we aim at providing the description of the anthropomorphic model, of the joints modeling, angle conventions and ranges of motions.

A. Skeletal model

The model includes 42 degrees of freedom (Table I), 18 joints and 19 segments. The pose (position and orientation) of a reference frame attached to the pelvis is expressed with respect an intertial world frame (Fig 1).

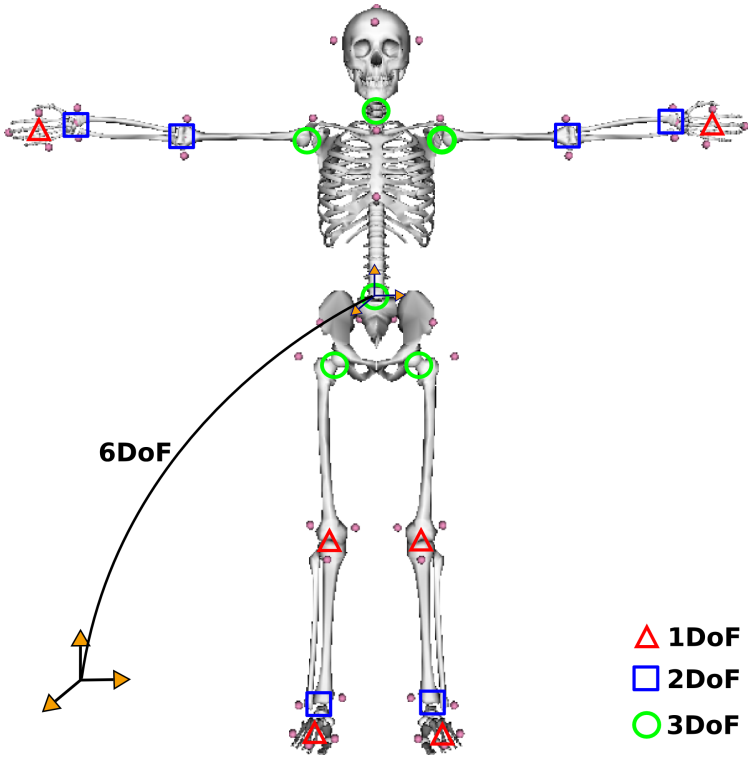

Fig. 1: Kinematics chain of the model. In order to model hinge joints (2 DoF), extra segments were added (talus and calcaneus, ulna and radius). The visual elements are based on the running model of Hammer [8].

The skeleton is modeled as a friction-less articulated multi-body dynamic system as shown in Fig 2. The pelvis, thighs, shanks and feet segments mass and inertia were set according to the model of [1] where data was obtained based on the studies of [14]. In this model, the length of the segments was taken from [5] model. The same model was used in [8] for simulating running motions. Upper limb anthropometry are based on the running model of [8] which was estimated based on the regression equations of [10] and [9]. Antrhopometry of the torso and head segments (including the neck) were estimated from the regression equations of [6], [7].

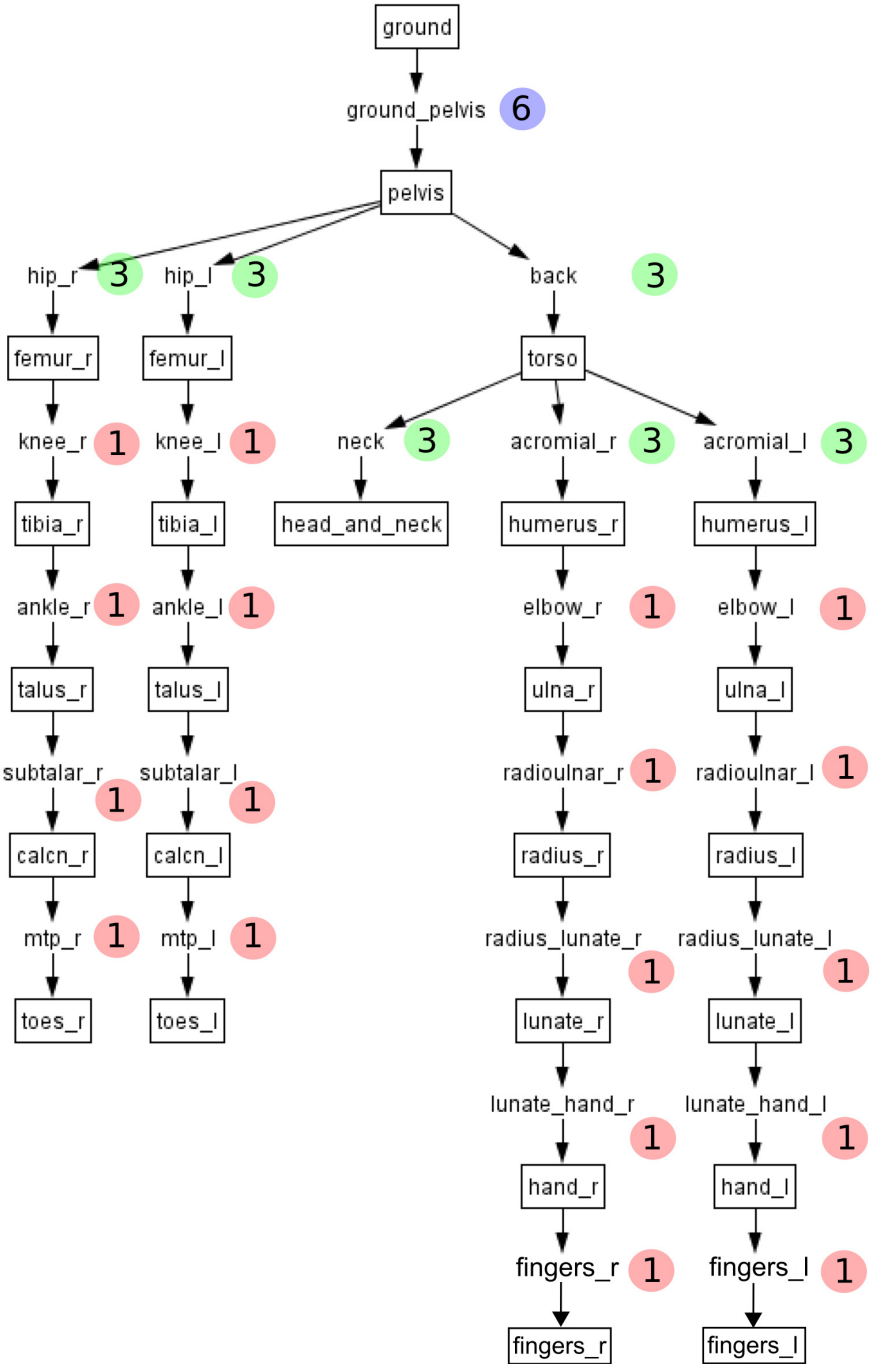

Fig. 2: Kinematics chain of the model. The numbers inside the colored balls indicate the number of degrees of freedom between segments. In order to model hinge joints (2 DoF) with Pinocchio, extra segments were added (talus and calcaneus, ulna and radius) to the model.

B. Joints modeling

The characteristics of the joint modeling are presented in Table I. Fig 2 show how joints are linked from parent to child segments in the kinematic chain. Euler XYZ body-fixed rotation angles are used to express the orientation using OpenSim.

The joint modeling adapted from the literature is described below:

- Each lower extremity has 7 DoF. The hip is modeled as a ball-and-socket joint, the knee is modeled as a hinge joint, the ankle is modeled as 2D hinge joints (flexion-extension and inversion-eversion), and the toes are modeled with one hinge joint at the metatarsals. Lower extremity joint definitions and the pelvis ones are based on [5] corrected in [2].
- The pelvis joint is modeled as a free-flyer joint to permit the model to translate and rotate in the 3D space. This 6D joint is attached to the free-floating base (root frame) of the under-actuated systems. The lumbar motion is modeled as a ball-and-socket joint and the neck joint is also modeled as a ball-and-socket joint. Joint definitions are based on [1].
- Each arm is modeled with 8 DoF. The shoulder is modeled as a ball-and-socket joint, the elbow and forearm rotations are modeled with hinge joints to represent flexion-extension and pronation-supination [9], the wrist flexion-extension and radial-ulnar deviations are modeled with hinge joints, and the hand fingers are modeled with one hinge joint for all fingers. Joint definitions are based on [8].

For further details about the location of each coordinate system with respect to bony landmarks, see [1].

Lower limb joints

	Hip	Knee	Ankle	Toes
Type	ball and socket	hinge	hinge (×2)	hinge

Upper limb joints

	Shoulder	Elbow	Wrist	Fingers
Type	ball and socket	hinge (×2)	hinge (×2)	hinge

Trunk and head joints

	Pelvis	Lumbar	Neck
Type	free flyer	ball and socket	ball and socket

TABLE I: Synovial joints and free flyer joint of the whole body model.

In the sequel we present some illustrations showing the ranges of motion of the model and the respective angle conventions.

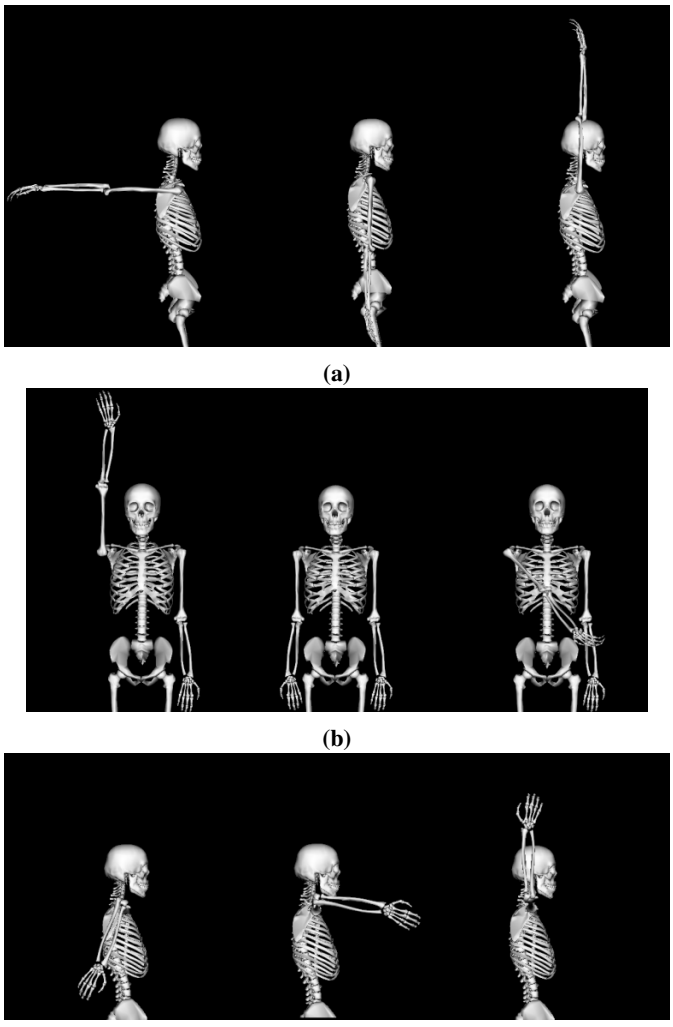

(a)

(b)

(c)

Fig. 3: **Shoulder joint conventions and range of motions.**
(a) Maximum shoulder extension (−) equal to 90 deg, anatomical pose and maximum shoulder flexion (+) equal to 180 deg.
(b) Maximum shoulder abduction (−) equal to 180 deg, anatomical pose and maximum shoulder aduction (+) equal to 35 deg.
(c) Maximum shoulder internal rotation (+) equal to 100 deg, anatomical pose and maximum shoulder external rotation (−) equal to 100 deg.

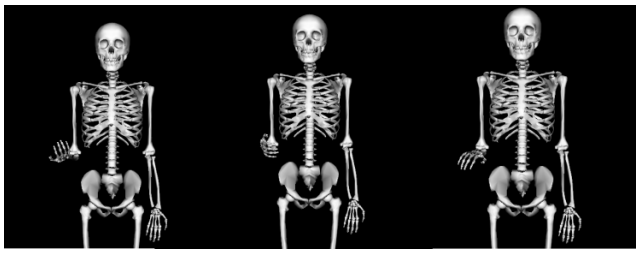

(a)

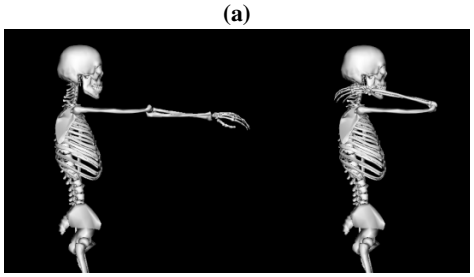

(b)

Fig. 4: **Elbow joint conventions and range of motions.**
(a) Maximum forearm supination equal to 110 deg, anatomical pose and maximum forearm pronation equal to 110 deg.
(b) Maximum elbow extension which is the same as the anatomical pose and maximum elbow flexion equal to 170 deg.

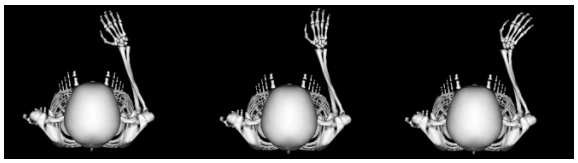

(a)

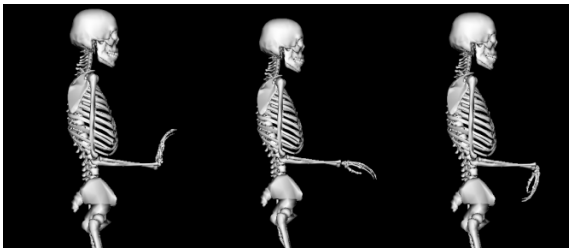

(b)

Fig. 5: **Wrist joint conventions and range of motions.**
(a) Maximum radial deviation equal to 25 deg, anatomical pose and maximum ulnar deviation equal to 35 deg.
(b) Maximum wrist extension equal to 90 deg, anatomical pose and maximum wrist flexion equal to 90 deg.

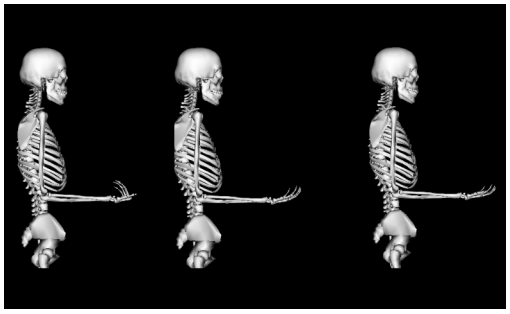

Fig. 6: **Fingers joint conventions and range of motions.**
(a) Maximum fingers flexion (+) equal to 90 deg, anatomical pose and maximum fingers extension (−) equal to 10 deg.

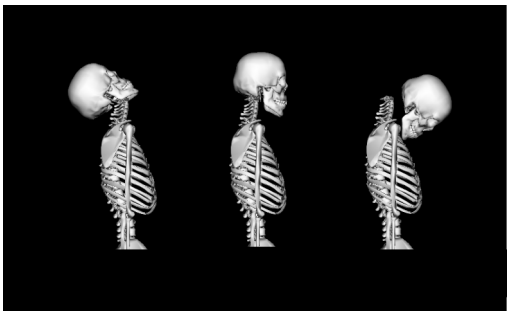

(a)

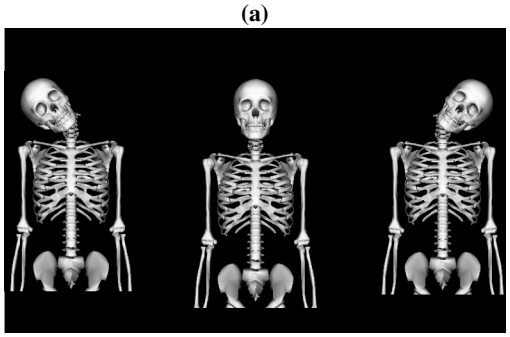

(b)

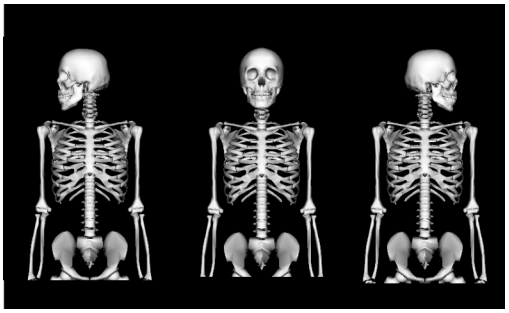

(c)

Fig. 7: **Neck joint conventions and range of motions.**
(a) Maximum neck extension (−) equal to 60 deg, the anatomical pose and maximum neck flexion (−) equal to 60 deg.
(b) Maximum neck right bending (+) equal to 45 deg, the anatomical pose and maximum neck left bending (−) equal to 45 deg.
(c) Maximum neck right rotation (−) equal to 80 deg, the anatomical pose and maximum neck left rotation (+) equal to 80 deg.

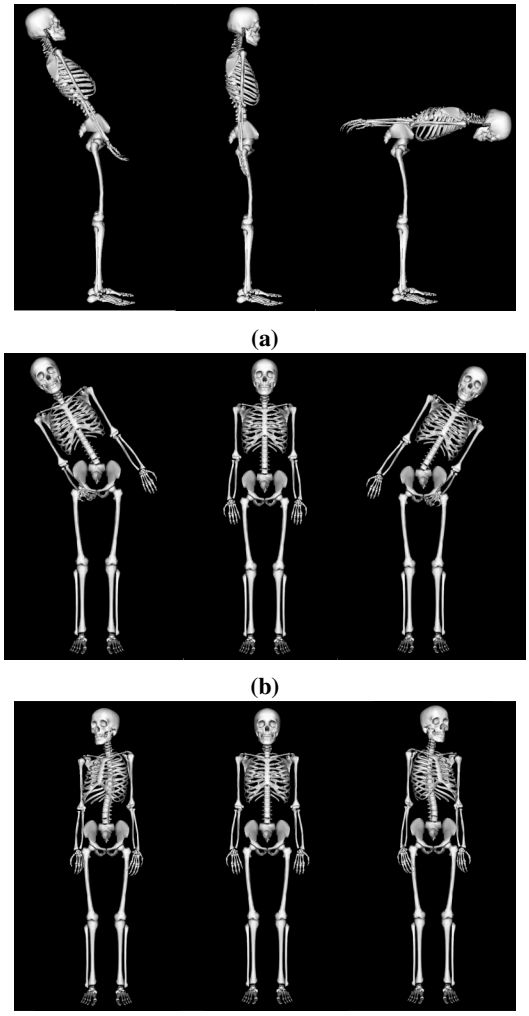

(a)

(b)

(c)

Fig. 8: **Lumbar joint conventions and range of motions.**
(a) Maximum lumbar extension (+) equal to 30 deg, anatomical pose and maximum lumbar flexion (−) equal to 90 deg.
(b) Maximum lumbar right bending (+) equal to 30 deg, anatomical pose and maximum lumbar left bending (−) equal to 30 deg.
(c) Maximum lumbar right rotation (−) equal to 30 deg, anatomical pose and maximum lumbar left rotation (+) equal to 30 deg.

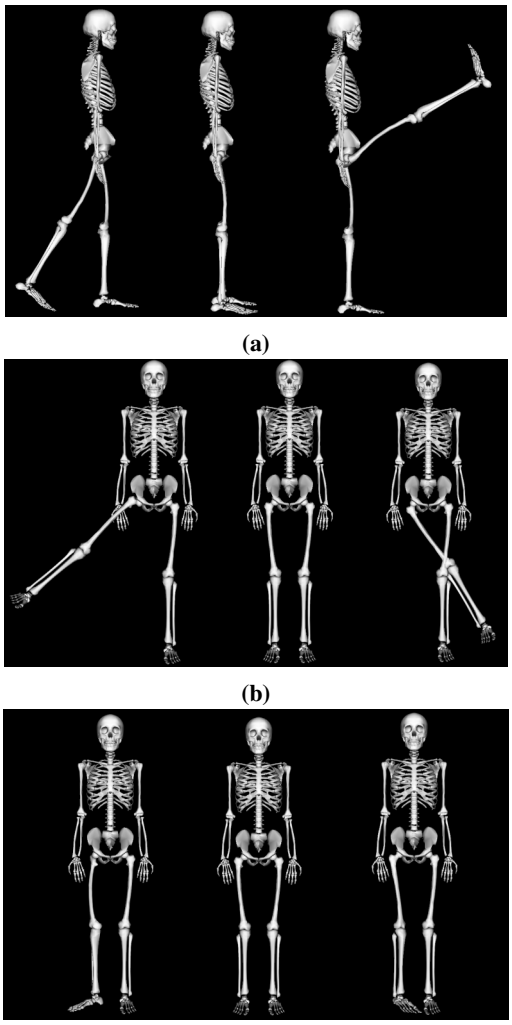

(a)

(b)

(c)

Fig. 9: **Hip joint conventions and range of motions.**
(a) Maximum hip extension (−) equal to 30 deg, anatomical pose and maximum hip flexion (+) equal to 120 deg.
(b) Maximum hip abduction (−) equal to 50 deg, the anatomical pose and maximum hip adduction (+) equal to 30 deg.
(c) Maximum hip external rotation (−) equal to 45 deg, the anatomical pose and maximum hip internal rotation (+) equal to 35 deg.

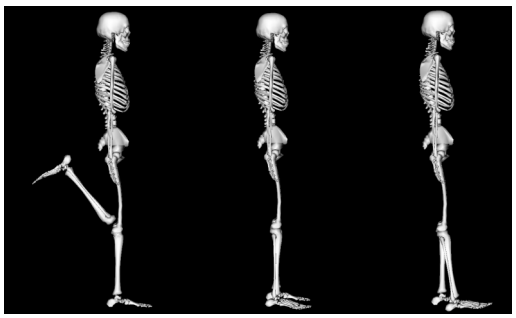

Fig. 10: **Knee joint conventions and range of motions.**
(a) Maximum knee flexion (−) equal to 140 deg, anatomical pose and maximum knee extension (+) equal to 10 deg.

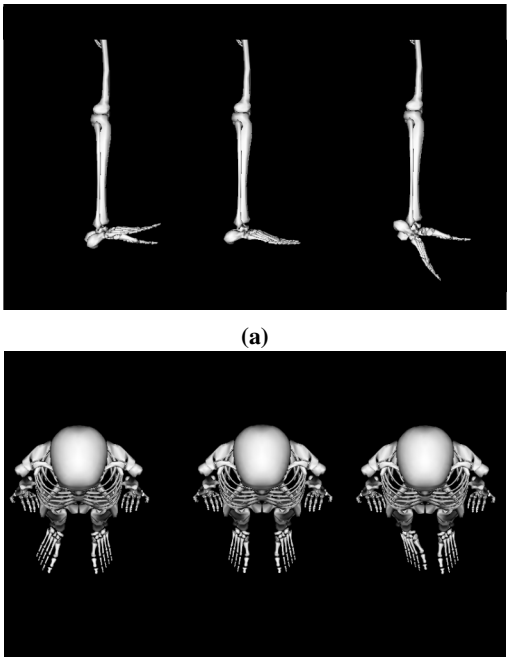

(a)

(b)

Fig. 11: **Ankle joint conventions and range of motions.**
(a) Maximum ankle dorsiflexion (+) equal to 20 deg, anatomical pose, maximum ankle plantarflexion (−) equal to 50 deg.
(b) Maximum ankle eversion (−) equal to 50 deg, anatomical pose and maximum ankle inversion (+) equal to 30 deg.

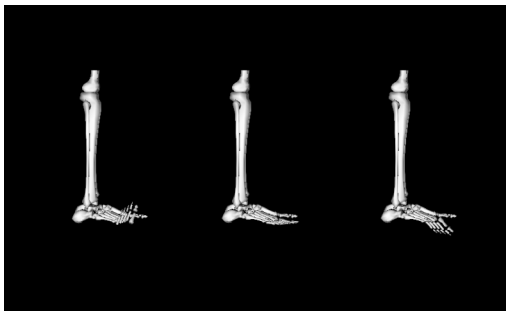

Fig. 12: **Toes joint conventions and range of motions.**
(a) Maximum toes extension (+) equal to 90 deg, anatomical pose and maximum toes flexion (−) equal to 45 deg.

III. Marker set

The model includes a whole-body marker set with 48 markers placed on anatomical bony landmarks (13) selected based on the recommendations of the International Society of Biomechanics (ISB) [17], [18].

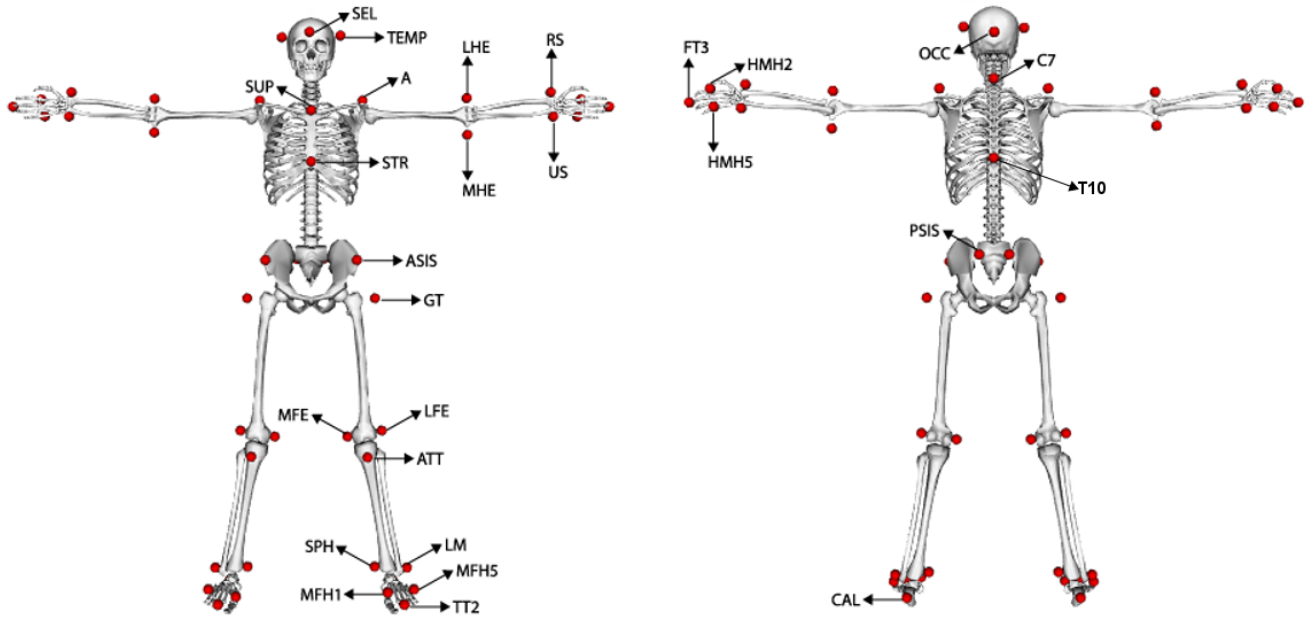

Fig. 13: Marker set depicted on the whole body skeletal model

Marker	Name	Location
SEL	Selenius	Between the eyebrows and above the nose.
OCC	Occipital	Back and lower part of the skull.
TEMP	Temporal	On the sides and base of the skull.
STR	Sternum	On the center of the chest.
A	Acromion process	Located on the lateral part of the shoulder, right above the shoulder joint.
C7	Seventh cervical vertebrae	Cervical area of the spinal cord.
T10	Tenth thoracic vertebrae	Thoracic area of the spinal cord.
SUP	Clavicle	Center of the clavicle.
LHE	Lateral humerus	Palpated on lateral sides of distal end of humerus.
MHE	Medial humerus	Palpated on medial sides of distal end of humerus.
US	Ulna	Long protuberance on lateral aspect of elbow.
RS	Radius	Long protuberance on medial aspect of elbow.
MH5	Fifth metacarpal	Long protuberance on proximal end of little finger metacarpal.
MH2	Second metacarpal	Long protuberance on proximal end of index finger metacarpal.
FT3	Middle finger	Over the tip of the medial finger.
ASIS	Antero superior ilac spine	Over the antero superior ilac spine.
PSIS	Posterior superior ilac spine	Over the posterior superior ilac spine.
GT	Greater trochanger	Lateral aspect of thigh just distal to hip joint.
LFE	Lateral femoral condyle	Lateral aspect on distal end of femur.
MFE	Medial femoral condyle	Medial aspect on distal end of femur.
ATT	Antero tibial tuberosity	Long protuberance on proximal end of femur.
SPH	Sphiron	Large protuberance on medial aspect of ankle.
LM	Lateral malleolus	Large protuberance on lateral aspect of ankle.
CAL	Calcaneus	Over the heel bone.
MFH1	Firs foot metatarsal	Long protuberance on proximal end of first toe metatarsal.
TT2	Second Toe	Long protuberance on second distal interphalangeal joint.
MFH5	Fifth foot metatarsal	Long protuberance on proximal end of first toe metatarsal.

TABLE II: Marker set

IV. Muscles modeling

The musculoskeletal model (Fig. 14) has been assembled to perform whole-body analysis of 3d human motion.

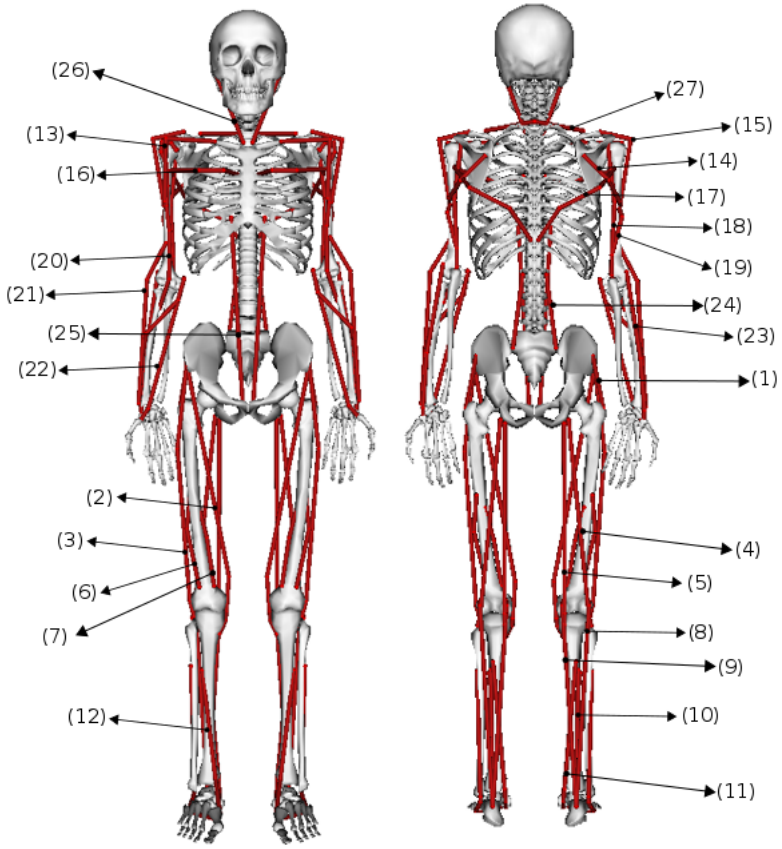

Fig. 14: Musculoskeletal model. The visual elements are based on the running model of Hammer [8].

The model contains 48 superficial muscles (Fig. 14) that represent the more relevant joint stabilizer muscles to study sport movements. The Muscles are modeled using hill-type models based on the works described in [15], [16] which are used in OpenSim [4]. The muscles and their principal mechanical actions in the execution of sport movements, are presented in Table III for the lower limb muscles, in Table IV for the upper limb muscles and in Table V for the trunk and head muscles.

A. Lower limbs muscles

Twenty three superficial muscles that stabilize the hip, knee and ankle joints were selected based on a functional analysis of the muscles mechanical action in the execution of jumps and landing techniques (Table III).

Lower limb muscles

Muscle	**Main Functions**
(1) Gluteus medius	Abduct an rotate medially the thigh at the hip.
(2) Sartorius	Flex, abduct, and rotate laterally the thigh at the hip. Flex the leg at the knee.
(3) Tensor fasciae latae	Extend the thigh at the hip.
(4) Biceps femoris	Flex and rotate the leg laterally at the knee. Extend the thigh at the hip.
(5) Semitendinoseus	Flex and rotate the leg medially at the knee. Extend the thigh at the hip.
(6) Vastus lateralis	Extend the leg at the knee.
(7) Vastus medialis	Extend the leg at the knee.
(8) Lateralis gastrocnemius	Plantar flex the foot at the ankle.
(9) Medialis gastrocnemius	Plantar flex the foot at the ankle and flex the leg at the knee.
(10) Soleus	Plantar flex the foot at the ankle.
(11) Tibialis posterior	Plantar flex the foot at the ankle. Slight inversion of the foot at the ankle.
(12) Tibialis anterior	Dorsiflex the foot at the ankle. Slight inversion of the foot at the ankle.

TABLE III: Lower body muscles of the whole body model and their mechanical action

B. Upper limbs muscles

Twenty one superficial muscles that stabilize the shoulder, elbow and wrist joints were selected based on a functional analysis of the muscles mechanical action in the execution of climbing techniques (Table IV).

Upper Limbs	
Muscle	**Main Functions**
(13) Anterior deltoideus	Abduction, flexion and medial rotation of the forearm at the shoulder joint
(14) Posterior deltoideus	Abduction, extension and lateral rotation of the upper arm at the shoulder joint
(15) Medial deltoideus	Abduction of the upper arm at the shoulder joint
(16) Pectoralis major	Flexion, adduction and medial rotation of the upper arm at the shoulder joint
(17) Latisimus dorsi	Extension, adduction, horizontal abduction, flexion from an extended position, and medial rotation of the upper arm at the shoulder joint
(18) Triceps brachii longus	Extension of the forearm at the elbow joint. Also adducts and may assist in extension of the shoulder joint.
(19) Triceps brachii lateralis	Extension of the forearm at the elbow joint.
(20) Biceps brachii longus	Supination and flexion of the forearm at the elbow joint.
(21) Brachioradialis	Flexion of the forearm at the elbow joint
(22) Carpi radialis flexor	Flexion and radial abduction of the hand at the wrist joint
(23) Carpialis extensor	Extension and radial abduction of the hand at the wrist joint.

TABLE IV: Upper body muscles of the whole body model and their mechanical action

C. Trunk and head muscles

Four superficial muscles that stabilize the lumbar and neck joints were selected based on a functional analysis of the muscles mechanical action in the execution of the sport techniques V. The sternocledomastoid and the trapecius ascendus muscles were used for studying the motion of the head. Nevertheless, the trapecius ascendus muscle is also important for the scapulae movement in the execution of climbing techniques.

Trunk	
Muscle	**Main Functions**
(24) Erector spinae longissimus	Extension of the lumbar spine at the lumbar joint
(25) Rectus abdominis	Flexion of the lumbar spine at the lumbar joint
(26) Sternocledomastoid	Oblique rotation and flexion of the head at the neck joint
(27) Trapecius ascendus	Scapulae motion and extension of the head at the neck joint

TABLE V: Trunk muscles of the whole body model and their mechanical action

REFERENCES

[1] Frank C Anderson and Marcus G Pandy. A Dynamic Optimization Solution for Vertical Jumping in Three Dimensions. *Computer Methods in Biomechanics and Biomedical Engineering*, 2(3):201–231, 1999.

[2] Edith M. Arnold, Samuel R. Ward, Richard L. Lieber, and Scott L. Delp. A model of the lower limb for analysis of human movement. *Annals of Biomedical Engineering*, 38(2):269–279, Feb 2010.

[3] Justin Carpentier, Florian Valenza, Nicolas Mansard, and Others. Pinocchio: fast forward and inverse dynamics for poly-articulated systems. https://stack-of-tasks.github.io/pinocchio, 2015.

[4] S. L. Delp, F. C. Anderson, A. S. Arnold, P. Loan, A. Habib, C. T. John, E. Guendelman, and D. G. Thelen. Opensim: Open-source software to create and analyze dynamic simulations of movement. *IEEE Transactions on Biomedical Engineering*, 54(11):1940–1950, 2007.

[5] S. L. Delp, J. P. Loan, M. G. Hoy, F. E. Zajac, E. L. Topp, and J. M. Rosen. An interactive graphics-based model of the lower extremity to study orthopaedic surgical procedures. *IEEE Transactions on Biomedical Engineering*, 37(8):757–767, Aug 1990.

[6] R. Dumas, L. Chèze, and J. P. Verriest. Adjustments to mcconville et al. and young et al. body segment inertial parameters. *Journal of Biomechanics*, 40(3):543–553, 2007.

[7] R. Dumas, L. Chèze, and J.-P. Verriest. Corrigendum to "Adjustments to McConville et al. and Young et al. body segment inertial parameters" [J. Biomech. 40 (2007) 543–553]. *Journal of Biomechanics*, 40(7):1651–1652, 2007.

[8] Samuel R. Hamner, Ajay Seth, and Scott L. Delp. Muscle contributions to propulsion and support during running. *Journal of Biomechanics*, 43(14):2709–2716, 2010.

[9] Katherine R S Holzbaur, Wendy M Murray, and Scott L Delp. A Model of the Upper Extremity for Simulating Musculoskeletal Surgery and Analyzing Neuromuscular Control. *Annals of Biomedical Engineering*, 33(6):829–840, 2005.

[10] Paolo De Leva. Adjustements to Zatsiorsky-Seluyanov's segment inertia paremeters. *Journal of Biomechanics*, 29(9):1223–1230, 1996.

[11] G. Maldonado, F. Bailly, P. Soueres, and B. Watier. Angular momentum regulation strategies for highly dynamic landing in parkour. *Computer Methods in Biomechanics and Biomedical Engineering*, 20(sup1):123–124, 2017. PMID: 29088618.

[12] Galo Maldonado, Philippe Soueres, and Bruno Watier. Strategies of parkour practitioners for executing soft precision landings. *Journal of Sports Sciences*, 0(0):1–7, 2018. PMID: 29690830.

[13] Galo Maldonado, Philippe Soueres, and Bruno Watier. From biomechanics to robotics. In Laumond Jean-Paul Watier Bruno Venture, Gentiane, editor, *Biomechanics of Anthropomorphic Systems*, volume 124. Springer International Publishing, In press 2019.

[14] J T. McConville, Clauser C. E., Kaleps I., Clauser C.R., and Cuzzi J. Anthropometric relationships of body and body segment moments of inertia. (Technical Report AFAMRL-TR-80-119), 1980.

[15] L. M. Schutte, M. M. Rodgers, F. E. Zajac, and R. M. Glaser. Improving the efficacy of electrical stimulation-induced leg cycle ergometry: an analysis based on a dynamic musculoskeletal model. *IEEE Transactions on Rehabilitation Engineering*, 1(2):109–125, Jun 1993.

[16] Darryl G Thelen. Adjustment of muscle mechanics model parameters to simulate dynamic contractions in older adults. *Journal of biomechanical engineering*, 2003.

[17] Ge Wu, Sorin Siegler, Paul Allard, Chris Kirtley, Alberto Leardini, Dieter Rosenbaum, Mike Whittle, Darryl D D'Lima, Luca Cristofolini, Hartmut Witte, Oskar Schmid, and Ian Stokes. ISB recommendation on definitions of joint coordinate system of various joints for the reporting of human joint motion—Part I: ankle, hip, and spine. *Journal of Biomechanics*, 35(4):543–548, 2002.

[18] Ge Wu, Frans C.T. van der Helm, H.E.J. (DirkJan) Veeger, Mohsen Makhsous, Peter Van Roy, Carolyn Anglin, Jochem Nagels, Andrew R. Karduna, Kevin McQuade, Xuguang Wang, Frederick W. Werner, and Bryan Buchholz. ISB recommendation on definitions of joint coordinate systems of various joints for the reporting of human joint motion—Part II: shoulder, elbow, wrist and hand. *Journal of Biomechanics*, 38(5):981–992, 2005.